



Published in final edited form as:

Kidney Int. 2018 March ; 93(3): 589–598. doi:10.1016/j.kint.2017.09.015.

Haploinsufficiency for *SIX2* increases nephron progenitor proliferation leading to elevated branching and nephron number.

Alexander N. Combes^{1,2,11}, Sean Wilson², Belinda Phipson², Brandon B. Binnie³, Adler Ju³, Kynan T. Lawlor², Cristina Cebrian⁴, Sarah L. Walton⁵, Ian M. Smyth^{6,7,8}, Karen M. Moritz⁵, Raphael Kopan⁹, Alicia Oshlack², and Melissa H. Little^{2,10,11}

¹Department of Anatomy & Neuroscience, University of Melbourne, VIC, Australia.

²Murdoch Children's Research Institute, Flemington Rd, Parkville, VIC, Australia

³Division of Cell Biology and Molecular Medicine, Institute for Molecular Bioscience, The University of Queensland, QLD, Australia

⁴Department of Internal Medicine, Division of Gastroenterology, University of Michigan, MI, USA

⁵School of Biomedical Sciences and the Centre for Child Health Research, The University of Queensland, QLD, Australia.

⁶Department of Biochemistry and Molecular Biology, Monash University, Wellington Rd, Clayton, Melbourne 3800, Australia.

⁷Monash Biomedicine Discovery Institute, 23 Innovation Walk, Monash University, Wellington Road, Clayton, Victoria 3800, Australia.

⁸Department of Anatomy and Developmental Biology, Monash University, 19 Innovation Walk, Clayton, Victoria 3800, Australia.

⁹Division of Developmental Biology, Cincinnati Children's Hospital Medical Center, OH, USA.

¹⁰Department of Paediatrics, The University of Melbourne, VIC, Australia.

Abstract

The regulation of final nephron number in the kidney is poorly understood. However, cessation of nephron formation occurs when the self-renewing nephron progenitor population commits to differentiation. Transcription factors within this progenitor population, such as *SIX2*, are assumed to control expression of genes promoting self-renewal such that homozygous *Six2* deletion results in premature commitment and an early halt to kidney development. In contrast, *Six2* heterozygotes were assumed to be unaffected. Using quantitative morphometry, we demonstrate here a

¹¹ Authors for correspondence: M.H.L.: +61 3 9936 6206; melissa.little@mcri.edu.au, A.N.C.: alexander.combes@unimelb.edu.au. Author contributions

S.W., B.B., A.J., K.T.L. & C.C. performed experiments and contributed to data analysis and presentation. B.P. and A.O. performed and advised on RNA-Seq analysis. S.L.W. & K.M. performed and advised on nephron counting. R.K. facilitated the *Fgf20* studies, I.M.S. facilitated access to OPT. A.N.C. conceived of the study with M.H.L., performed experiments, analysed and presented the data and wrote the manuscript. M.H.L. supervised the study and substantially contributed to writing. All authors contributed to revising and editing the manuscript.

Statement of competing financial interests

Disclosures: None

paradoxical 18% increase in ureteric branching and final nephron number in *Six2* heterozygotes, despite evidence for reduced levels of SIX2 protein and transcript. This is accompanied by a clear shift in nephron progenitor identity with a distinct subset of progenitor genes, including *Cited1* and *Meox1*, downregulated, while others were unaffected. The net result was an increase in nephron progenitor proliferation, as assessed by elevated EDU labelling, an increase in MYC protein and transcriptional upregulation of MYC target genes. Reducing proliferation by introducing *Six2* heterozygosity onto the *Fgf20*^{-/-} background resulted in premature differentiation of the progenitor population. Overall, this data demonstrates a unique dose response of the nephron progenitors to the level of SIX2 protein in which the role of SIX2 in progenitor proliferation versus self-renewal is separable.

Introduction

Nephron number varies in both human and mouse with pathological consequences for individuals on the lower end of the spectrum.¹ Nephrons are induced to form from a self-renewing nephron progenitor population, which promotes branching in the adjacent ureteric tip, and responds to tip-produced signals to form nephrons.² Limiting the number of nephron progenitors by restricting FGF signalling,³ or ablating a portion of the progenitor population,⁴ reduces final nephron number. Conversely, preventing progenitor differentiation shortly after birth by chemical inhibition of SMAD signalling resulted in a modest increase in nephron number.⁵ Thus, regulating the balance of progenitor self-renewal and differentiation has a significant bearing on nephron endowment.

The transcription factor, SIX2, which is expressed in the nephron progenitor (NP) population of the developing kidney in both mouse and man, plays a central role in maintaining a functional pool of self-renewing NPs.^{6, 7} SIX2 has assumed to act by suppressing differentiation and driving self-renewal of the nephron progenitors. Homozygous loss of *Six2* in mice causes a global and early onset loss of self-renewal and premature differentiation of NPs.⁷ This early loss of progenitors severely reduces organ size as it is also the NP population that drives ureteric branching via the production of factors such as GDNF.⁸ Conversely, overexpression of *Six2* in mice prevents NP differentiation.⁹ Genome-wide binding studies in mouse and human have been used to identify hundreds to thousands of genomic loci potentially regulated by SIX2^{10, 11}. As these include genes expressed in NPs and resulting nephrons, the assumption is that SIX2 can both activate and suppress transcription. Evidence for binding of SIX2 to its own promoter also suggested an autoregulatory feedback loop.¹²

Cellular heterogeneity within the nephron progenitor population is evident in variations in the level of expression of genes including *Cited1* and *Meox1*, with an assumption that *Cited1*⁺*Six2*⁺ CM cells are less committed than CM cells expressing *Six2* alone.^{13, 14} Indeed, we have demonstrated that SIX2 levels within individual nephron progenitor cells appears to correlate with variation in cell cycle length; high SIX2 is associated with slower-cycling CM cells while lower SIX2 levels are seen in faster-cycling CM cells closer to the site of nephron formation.¹⁵ One interpretation of this observation is that the progenitor population is gradually progressing from an uncommitted to a committed state as SIX2

protein levels change. Despite this, the *Six2* heterozygous state has been regarded as having normal kidney development. Indeed, the *Six2*^{GCE/+} mouse line (*Six2*^{GCE/+})⁶ is heterozygous for *Six2* but has been used in a number of studies to conditionally delete genes within nephron progenitors on the assumption that the background phenotype is wildtype.^{10, 16–21}

Given the importance of *Six2* in nephron progenitor regulation, we used multiscale imaging and transcriptional profiling to more carefully examine this *Six2*^{GCE/+} mouse strain. As *Six2* knockout mice show a complete collapse of kidney development, we anticipated an intermediate phenotype between a wildtype and *Six2* null. While reduced SIX2 protein was evident in the kidneys of *Six2*^{GCE/+} mice, contrary to expectations, branching and nephron number was increased. At the transcriptional level, no change was observed for some markers of CM identity, including *Sall1*, *Pax2*, *Wt1* and *Gdnf*, however there was a clear reduction in a distinct subset of CM genes previously associated with the most progenitor-like SIX2^{Hi} nephron progenitor population. This shift in nephron progenitor heterogeneity resulted in a global increase in progenitor proliferation accompanied by evidence for increased MYC protein and MYC pathway activity. As such, this suggests a bimodal response of the developing kidney to SIX2 protein levels and suggests a previously unappreciated dose and target-sensitive separation between the role of SIX2 in self-renewal and progenitor proliferation.

Results

Increased branching, proliferation and nephron number in *Six2*^{GCE/+} mice

We first investigated whether the *Six2*^{GCE/+} was haploinsufficient by qPCR and Western blotting of whole 15.5 days post coitum (dpc) embryonic kidneys. This revealed a reduction of both *Six2* transcript and SIX2 protein by ~50% in *Six2*^{GCE/+} mice compared to *Six2*^{+/+} controls (Fig. 1A-F, Supplementary Fig.1). Expression of *Cited1*, a marker of the uncommitted NP subpopulation, was reduced by 70% in *Six2*^{GCE/+} mice (Fig1G). Comparison of isolated NPs from *Six2*^{GCE/+} and *Six2*^{+/+} kidneys was not feasible without introducing an additional reporter to label wildtype NPs, which may have had phenotypic consequences. For example, another common NP reporter, the *Six2*TGC BAC transgenic reporter has a distinct heterozygous phenotype independent of the *Six2* locus (unpublished data). Based on the phenotype of the total *Six2* knockout, we speculated that reducing *Six2* levels would result in increased differentiation and a decrease in branching. Potential changes in branching were assessed with optical projection tomography by measuring the number of NP fields (niche number), which reports the amount of branching in the whole organ.^{15, 22} Counter to expectations, niche number was increased in *Six2*^{GCE/+} compared to *Six2*^{+/+} kidneys (23% at 15.5 dpc, 14% at 19.5 dpc/ postnatal day (P) 0 and 18% at P2; Fig. 2A,B). Confocal analysis did not detect a significant reduction in the average number of NP and tip cells per niche at 15.5 dpc (Fig. 2C,D). Multiplying the average number of NPs per niche by niche number reflects a 10% increase in the NP population at 15.5 dpc. We have previously characterised the rate of branching across time and found that the most rapid phase of branching occurs before 15.5dpc¹⁵ so a transient increase in the progenitor population at and before this time could drive a lasting increase in branching even if the total number of progenitors decreases later in development. By P0, the number of NP cells per

niche and the total NP population was reduced by ~10% while tip cell number was unchanged (Fig. 2C,E). The decrease in NP cells per niche at this stage could reflect a faster rate of NP differentiation, in line with reduced *Cited1* expression in *Six2*^{GCE/+}, however the timing of cessation of nephron formation was not altered. NP were present at P2 (Fig. 2A) and had differentiated by P4 (data not shown) in *Six2*^{GCE/+} and controls. EdU incorporation at 13.5 dpc revealed a significant increase in NP and tip cell proliferation (Fig. 2F). Unbiased stereology was used to determine whether the increased branching and NP population size resulted in an increase in final glomerular number. At P21, total glomerular counts were increased by 18% in *Six2*^{+/-GCE} (Fig. 2G). As the number of nephrons per tip at P4 was unchanged (data not shown), increased final nephron number was associated with increased branching rather than an increase in the number of nephrons forming around each tip.

Transcriptional comparison between *Six2*^{+/-}, *Six2*^{GCE/+} and *Six2*^{GCE/GCE} kidneys

The global transcriptional changes observed in the *Six2* homozygous or heterozygous state have not previously been examined. To examine the transcriptional response to changes in *Six2* levels, whole kidney RNA-Seq was performed on *Six2*^{GCE/+} and *Six2*^{+/-} kidneys at 15.5 dpc as well as *Six2*^{+/-}, *Six2*^{GCE/+} and *Six2*^{GCE/GCE} at 11.5 dpc (Supplementary table 1). As expected, *Six2* mRNA levels in *Six2*^{GCE/+} were ~50% of wildtype. The top differentially expressed genes from RNA-seq at 11.5 and 15.5 were cross-validated by real time PCR (Supplementary Fig. 2). The *Six2*^{GCE/+} construct drives the expression of GFP and Cre recombinase in place of the native *Six2* transcript.⁶ To test the possibility that the transcriptional and phenotypic changes observed in this strain resulted from the expression of recombinant GFP-CreERT2 within the NPs, qPCR for genes both up- and down-regulated in *Six2*^{GCE/+} kidneys was performed in kidneys from *Gdnf*^{CreERT2} mice.⁴ These genes were not differentially expressed in the *Gdnf*^{CreERT2} line (Supplementary Fig. 3), consistent with a specific response to *Six2* haploinsufficiency.

Six2^{GCE/+} kidneys display altered expression in only a subset of NP markers and previously described SIX2 targets

A subset of genes were downregulated in the *Six2*^{GCE/+} at 15.5 dpc (vice versa for upregulated genes) (Fig. 3A). At 11.5dpc, genes including *Cited1* (0.38 FC) and *Crym* (0.40 FC) were already downregulated in 11.5 dpc *Six2*^{GCE/GCE} (Fig. 3C). This represents a dose-sensitive (haploinsufficient) response pattern, and included *Cited1* (0.33FC at 15.5dpc), *Meox1* (0.70 FC), *Crym* (0.59 FC), *Hoxd12* (0.72 FC), and *Phf19* (0.74 FC).^{14, 23–27} Most of these represent genes previously identified as marking a subset of the NP population regarded as the most uncommitted. Considering all differentially regulated genes, these were enriched for genes known to be expressed in NP and predicted to be regulated by SIX2. Of the 40 genes significantly downregulated at 15.5dpc in the *Six2*^{GCE/+} state, 83% represented NP markers and 65% associated with a previously described SIX2 binding site.^{10, 11} GO analysis²⁸ of downregulated genes revealed a link to metabolism and negative regulation of glycolysis, consistent with a change in proliferative capacity and the previously described role for SIX proteins in regulating myogenesis²⁹ (Supplementary Table 2). Of the 13 upregulated genes at 15.5dpc, 9 were previously associated with a SIX2 ChIP peak and 7 were expressed in the NPs. A similar pattern was observed at 11.5dpc (Fig. 3B).

Despite evidence for a clear transcriptional effect within the NP population even in the heterozygous state, many NP genes and previously proposed SIX2 target genes showed no change in expression in the 15.5dpc *Six2*^{GCE/+} kidney. For example, *Gdnf*, *Wnt4*, and *Fgf8*, all previously proposed as direct SIX2 target genes,^{7, 10–12} were not significantly changed, while *Eya1*, was only moderately upregulated (1.2 FC adj p = 8.3E-6) (Fig. 3C). In addition, while branching was increased, no substantial changes were observed in genes associated with the regulation of branching morphogenesis or NP-stroma interactions (Fig. 3C, and data not shown). This would suggest that many genes affected by total deletion of *Six2* were insensitive to this reduced level of protein.

Evidence for differential dose-sensitivity in *Six2* target genes

Comparison of transcriptional changes in the homozygous state compared to wildtype (Fig. 4A), provided an opportunity to validate a role for *Six2* in the regulation of previously proposed target genes. Comparing all differentially expressed genes in *Six2*^{GCE/GCE} kidneys (adjusted p<0.05, no fold change cutoff) to genes associated with SIX2 binding in mouse^{10, 11} revealed that only 8.8% of potential SIX2 targets responded to complete loss of SIX2 protein *in vivo*. A complete description of the transcriptional response observed in the homozygous state can be found in supplementary data. Indeed, by identifying the overlapping genes showing differential regulation in both the heterozygous and homozygous state at 11.5dpc, it is possible to identify those genes most sensitive to reduced levels of SIX2 protein. Again, this highlights those genes previously identified as marking the most uncommitted cell domain with the NP as being the most sensitive to SIX2 protein levels. However, while reduced expression of these genes is associated with loss of NP self-renewal / increased NP commitment in the homozygote state, in the heterozygous state this was accompanied by increased NP niche number and increased ureteric branching.

Increased CM proliferation is associated with elevated MYC protein levels in *Six2* haploinsufficient kidneys

As the *Six2*^{GCE/+} phenotype results in a larger kidney with a more proliferative NP population, we looked for evidence of a proliferative signature within the differentially expressed genes at 15.5dpc. One of the genes most significantly down regulated at both 15.5dpc and 11.5dpc (0.42 and 0.53 FC respectively) was *Actn3b*. ACTN3B protein levels were also reduced by >50% at 15.5 dpc in *Six2*^{GCE/+} (Supplementary Fig. 2). This decrease in ACTN3B is associated with an increase in metabolic efficiency, also likely to influence progenitor proliferation.³⁰ In addition, genes differentially expressed between the *Six2*^{GCE/+} versus *Six2*^{+/+} kidney at 15.5dpc were tested for enrichment of the Broad Institute's Hallmark gene sets using the CAMERA gene set test.³¹ At 15.5 dpc, upregulated genes were significantly enriched in pathways associated with mTORC1 signalling, and MYC target genes (Fig. 4B). These results were confirmed at 11.5 dpc with an additional signature for PI3K-AKT-MTOR signalling (Fig. 4B, Supplementary table 2). While *Myc* is associated with SIX2 binding and therefore potentially regulated by SIX2¹⁰, *Myc* mRNA was not upregulated in the whole kidney data. However, using Western blotting, we could confirm that MYC protein levels were increased by 19% in *Six2*^{GCE/+} compared to *Six2*^{+/+} across multiple litters (p=0.009) (Fig. 4C). EYA1, SIX2 and MYC have been proposed to cooperatively regulate NP expansion, with SIX2 mediating EYA1 nuclear translocation, and

EYA1 dephosphorylating MYC T58 to prevent protein degradation and promote progenitor expansion.³² However, in *Six2*^{GCE/+} mice, *Eya1* mRNA levels were only increased 1.2 fold at 15.5 dpc and there was no difference in MYC T58 phosphorylation or the prevalence of T58 positive cells within the NP by immunofluorescence (Supplementary Fig. 4). This suggests a different mechanism for elevation of MYC protein. Investigation of the mTOR pathway and PI3kinase-p110-alpha protein levels failed to detect any significant change (Supplementary Fig. 4). Thus, the changes in NP proliferation are most likely driven by an increase in MYC protein levels either directly or indirectly due to changes in SIX2 protein levels.

Six2 heterozygous nephron progenitors are compromised with respect to self-renewal

Although *Six2*^{GCE/+} kidneys branched more than *Six2*^{+/+}, it remained possible that the *Six2*^{GCE/+} NP domain represents a sensitised progenitor state. The distinction between the heterozygous and homozygous *Six2* knockout stems from an elevated NP proliferation in the former. *Fgf9* and *Fgf20* are known to be critical for NP survival and proliferation.³ Kidneys from *Fgf20*^{-/-} mice display reduced NP proliferation and reduced niche thickness around birth but otherwise appear normal.³ More careful quantitation of kidney morphogenesis in the *Fgf20*^{-/-} mice by optical projection tomography showed a 15% reduction in ureteric branching (Supplementary Fig. 5). These mice were then crossed with the *Six2*^{GCE/+} strain and the expression of *Six2* and *Cited1* examined across all potential genotypes (Supplementary Fig. 5). While removal of one or both copies of *Fgf20* did not result in a further reduction in *Six2* levels, *Six2*^{GCE/+}*Fgf20*^{-/-} kidneys were severely hypoplastic and depleted of nephron progenitors by 15.5 dpc (Fig. 5A,B). At 12.5 dpc, *Six2*^{GCE/+}*Fgf20*^{-/-} kidneys had weak SIX2 expression and ectopic renal vesicles forming around most tips (Fig. 5 C-H), reminiscent of the *Six2* knockout⁷. While FGF signalling plays an important role in NP maintenance, the lack of further reduction of *Six2* levels in the *Six2*^{GCE/+}*Fgf20*^{-/-} suggests *Fgf20* is not directly regulating *Six2* levels. *Fgf20* on the other hand is bound by SIX2¹⁰ and substantially downregulated in the *Six2*^{GCE/GCE}. These results primarily show that *Six2*^{GCE/+} NPs are sensitised to differentiation as *Fgf20* deletion alone does not result in this phenotype. This is functional evidence that NP state is compromised and is an important caution to future studies that may assume that this inducible Cre will not affect an experimental outcome.

Discussion

This study not only reveals a clear kidney phenotype in *Six2* heterozygous mice, but a paradoxical increase in nephron number and branching events despite clear evidence of a transcriptional dysregulation of a subset of SIX2 target genes. This variation in phenotype from wildtype to heterozygote to homozygote suggests a dose-sensitive separation between the regulation of NP proliferation versus self-renewal. What is evident is that as SIX2 protein levels decline, inhibition of NP proliferation is relaxed prior to a loss of NP self-renewal. As a result, the NP population expands as a consequence of increased proliferation mediated in part by increased MYC protein and MYC pathway signalling. This expanded NP population drives increased branching apparently without any requirement for an overall upregulation of GDNF expression levels but simply an increase in the number of NP cells

present. As SIX2 protein levels fall further, the loss of regulation of self-renewal is affected, tipping the NP population into nephron commitment.⁷ This immediately blocks branching by reducing the size of the NP population. Of interest, what we did not observe is a change in the timing of cessation of nephrogenesis in the *Six2* heterozygous state. As is seen in the wildtype situation, the NP eventually reduced in cell number per niche. The overall increase in nephron number in this genotype, therefore, suggests that each tip was able to generate a normal number of nephrons, supporting a genuine expansion of the progenitor pool without a change in the timing of cessation.

Expansion of the progenitor pool in *Six2*^{GCE/+} was clearly driven by increase in NP proliferation, with evidence of elevated EdU labelling, increased MYC protein levels and hallmarks of increased MYC pathway activity. Even modest increases in MYC levels have previously been shown to promote dose-dependent expansion of cell populations in fly and mouse^{33, 34} and to expand human pluripotent cardiac progenitors.³⁵ MYC has previously been shown to regulate NP turnover and deletion of MYC within the NP domain reduces NP number and kidney volume.^{32, 36} The increase in progenitor proliferation in *Six2*^{GCE/+} may also be complemented by the de-repression or compensatory upregulation of *Fgf1*, *Adra1*, and *Klhdc8a*, all of which were upregulated in the heterozygous state by 15.5dpc and all of which are associated with SIX2 binding,¹⁰ and increased growth in other contexts.^{37, 38}

This study has identified a high correlation between differentially expressed genes in the *Six2*^{GCE/+} with genes that associate with SIX2 binding.^{10, 11} However, it has also revealed some unexpected findings. Established SIX2 targets *Gdnf* and *Wnt4* were not affected by reduced SIX2 protein levels. Even in the *Six2* null, there was only a modest reduction in SIX2 target genes *Gdnf* and *Eya1*, indicating that SIX2 is not the only regulator of these genes. The *Six2* locus itself has a documented autoregulatory element¹⁰⁻¹² which did not maintain *Six2* expression levels in the heterozygous state. *Six2* is proposed to silence drivers of early nephrogenesis, including *Wnt4* and *Fgf8*.¹¹ *Wnt4* was upregulated in the *Six2*^{GCE/GCE}, but *Fgf8* was unchanged. In contrast, multiple genes previously identified as WT1 targets²⁶ were among the top downregulated genes in the *Six2*^{GCE/GCE}, consistent with a model in which nephron progenitor maintenance is regulated by multiple transcription factors working redundantly on a set of core target genes.

The observed increase in nephron number in *Six2* heterozygotes has implications for our understanding of congenital anomalies of the kidney and urinary tract (CAKUT) in humans. Despite an initial association between heterozygous *Six2* mutations and a renal phenotype,³⁹ subsequent analysis of large cohorts of CAKUT patients cast doubt on the clinical relevance of some reported mutations, and failed to identify any new associations with *Six2*.^{40, 41} This is consistent with a high likelihood of functional redundancy between SIX1 and SIX2 in human, which unlike in mouse, are co-expressed in nephron progenitors.¹⁰ The data presented here would not predict any pathogenicity from a heterozygous mutation in *Six2*. It should also be noted that the *Six2*^{GCE/+} strain is also used for conditional deletion of other genes and lineage tracing.^{10, 16-21} An interaction between the *Six2*^{GCE/+} phenotype and experiments using this line should be considered when interpreting these studies. As demonstrated with the *Six2*^{GCE/+} *Fgf20*^{-/-} cross, *Six2* heterozygosity has the capacity to exacerbate otherwise modest phenotypes.

In summary, we provide evidence here for distinct phenotypes dependent upon the amount of SIX2 protein present within the NP of the developing kidney. As a result of differential target gene sensitivity, haploinsufficiency for *Six2* caused a paradoxical increase in NP proliferation and increased nephron number in contrast to the loss of the NP population in the absence of *Six2*. However, the *Six2* heterozygous NP population is sensitised as a reduction in NP proliferation, generated by crossing this line onto the *Fgf20*^{-/-} strain, shifted the balance to loss of self-renewal. Importantly, while the concept that reduced progenitor number results in less nephrons is accepted, we provide evidence that the converse is also true. A better understanding of how to positively control nephron progenitor expansion *in vivo* may have therapeutic implications for improving developmental outcomes and in generating renal tissue *in vitro*.

Concise methods

Mouse Strains and Embryo Staging

In all experiments, noon of the day on which the mating plug was observed was designated 0.5 *days post coitum* (dpc). For postnatal samples, P was recorded with P0 equivalent to birth. In most instances, birth represented 19.5 dpc. *Six2*^{GCE/+} mice were used, which carry a targeted insertion of EGFP-CRE-ERT2 in the *Six2* locus that generates a null allele (JAX stock number 009600)⁶. *Fgf20*-null mice (*Fgf20*^{β-gal})⁴² were kindly provided by David Ornitz. All animal experiments in this study were assessed and approved by the University of Queensland or Murdoch Children's Research Institute Animal Ethics Committees and were conducted under applicable Australian laws governing the care and use of animals for scientific purposes.

Immunofluorescence and image analysis

The following primary antibodies were used: mouse anti-calbindin D28K (Sigma-Aldrich C9848), mouse anti-cytokeratin (Abcam Ab11213 and Ab115959), rabbit anti-SIX2 (Proteintech 11562-1-AP), rabbit anti-JAG1 (Abcam ab7771), mouse anti-SIX2 (Abnova H00010736-MO1), rat anti-Ecad (Invitrogen 13-1900). The mouse SIX2 primary was used in conjunction with an isotype-specific secondary antibody (Life technologies A21121) to reduce background staining. Alexa Fluor-conjugated secondary antibodies (Life Technologies) were used to detect primary antibodies and DAPI (Sigma-Aldrich D8417) was used at 1:2000 to label nuclei. Whole mount immunofluorescence, confocal microscopy, and optical projection tomography was carried out according to published protocols²². Cell counts per niche (confocal) and niche counts (OPT) were performed as reported²². Quantitative analysis of SIX2 fluorescence intensity is detailed in supplementary methods.

Proliferation analysis

Relative amounts of proliferation were investigated by analysis of EdU incorporation in CM and ureteric tip, 30 min after exposure to EdU as assessed by whole mount confocal imaging and quantitative analysis as reported¹⁵. A total of 8 *Six2*^{+/+} and 9 *Six2*^{+/GCE} kidneys were assessed, each from an individual animal, from three separate timed pregnancies.

Glomerular estimation

Glomerular number was estimated using the physical disector/fractionator method as previously described⁴³, further detail provided in supplementary methods.

Transcriptional profiling using RNA-Seq & Western Blotting

Experimental information and analysis workflow for RNA Seq and Western blotting is detailed in supplementary methods.

Supplementary Material

Refer to Web version on PubMed Central for supplementary material.

Acknowledgements

This work was supported by the Australian Research Council (DE150100652), the National Health and Medical Research Council of Australia (APP1002748, APP1063696), the Human Frontiers in Science Program (RGP0039/2011). Microscopy was performed at the ACRF/IMB Cancer Biology Imaging Facility, which was established with the support of the Australian Cancer Research Foundation, at Monash University, and at the Murdoch Children's Research Institute. A.N.C. holds a Discovery Early Career Researcher Award from the Australian Research Council. M.H.L. is a Senior Principal Research Fellow of the NHMRC. We thank the IMB Sequencing Facility for NGS services, David Ornitz for the *Fgf20* mice, Kieran Short, Lynelle Jones, Shireen Lamande, Chantal Coles, and Peter Houweling for technical assistance. MCRI is supported by the Victorian Government's Operational Infrastructure Support Program.

References

1. Hoy WE, Hughson MD, Bertram JF, et al. Nephron number, hypertension, renal disease, and renal failure. *Journal of the American Society of Nephrology : JASN* 2005; 16: 2557–2564. [PubMed: 16049069]
2. Kopan R, Chen S, Little M. Nephron progenitor cells: shifting the balance of self-renewal and differentiation. *Current topics in developmental biology* 2014; 107: 293–331. [PubMed: 24439811]
3. Barak H, Huh SH, Chen S, et al. FGF9 and FGF20 maintain the stemness of nephron progenitors in mice and man. *Developmental cell* 2012; 22: 1191–1207. [PubMed: 22698282]
4. Cebrian C, Asai N, D'Agati V, et al. The number of fetal nephron progenitor cells limits ureteric branching and adult nephron endowment. *Cell reports* 2014; 7: 127–137. [PubMed: 24656820]
5. Brown AC, Muthukrishnan SD, Oxburgh L. A synthetic niche for nephron progenitor cells. *Developmental cell* 2015; 34: 229–241. [PubMed: 26190145]
6. Kobayashi A, Valerius MT, Mugford JW, et al. Six2 defines and regulates a multipotent self-renewing nephron progenitor population throughout mammalian kidney development. *Cell stem cell* 2008; 3: 169–181. [PubMed: 18682239]
7. Self M, Lagutin OV, Bowling B, et al. Six2 is required for suppression of nephrogenesis and progenitor renewal in the developing kidney. *The EMBO journal* 2006; 25: 5214–5228. [PubMed: 17036046]
8. Combes AN, Davies JA, Little MH. Cell-cell interactions driving kidney morphogenesis. *Current topics in developmental biology* 2015; 112: 467–508. [PubMed: 25733149]
9. Chung E, Deacon P, Marable S, et al. Notch signaling promotes nephrogenesis by downregulating Six2. *Development* 2016.
10. O'Brien LL, Guo Q, Lee Y, et al. Differential regulation of mouse and human nephron progenitors by the Six family of transcriptional regulators. *Development* 2016; 143: 595–608. [PubMed: 26884396]
11. Park JS, Ma W, O'Brien LL, et al. Six2 and Wnt regulate self-renewal and commitment of nephron progenitors through shared gene regulatory networks. *Developmental cell* 2012; 23: 637–651. [PubMed: 22902740]

12. Brodbeck S, Besenbeck B, Englert C. The transcription factor Six2 activates expression of the Gdnf gene as well as its own promoter. *Mechanisms of development* 2004; 121: 1211–1222. [PubMed: 15327782]
13. Brown AC, Muthukrishnan SD, Guay JA, et al. Role for compartmentalization in nephron progenitor differentiation. *Proceedings of the National Academy of Sciences of the United States of America* 2013; 110: 4640–4645. [PubMed: 23487745]
14. Mugford JW, Yu J, Kobayashi A, et al. High-resolution gene expression analysis of the developing mouse kidney defines novel cellular compartments within the nephron progenitor population. *Developmental biology* 2009; 333: 312–323. [PubMed: 19591821]
15. Short KM, Combes AN, Lefevre J, et al. Global quantification of tissue dynamics in the developing mouse kidney. *Developmental cell* 2014; 29: 188–202. [PubMed: 24780737]
16. Taguchi A, Kaku Y, Ohmori T, et al. Redefining the in vivo origin of metanephric nephron progenitors enables generation of complex kidney structures from pluripotent stem cells. *Cell stem cell* 2014; 14: 53–67. [PubMed: 24332837]
17. Yuri S, Nishikawa M, Yanagawa N, et al. Maintenance of Mouse Nephron Progenitor Cells in Aggregates with Gamma-Secretase Inhibitor. *PloS one* 2015; 10: e0129242. [PubMed: 26075891]
18. Togel F, Valerius MT, Freedman BS, et al. Repair after nephron ablation reveals limitations of neonatal nephrogenesis. *JCI insight* 2017; 2: e88848. [PubMed: 28138555]
19. Xu J, Liu H, Park JS, et al. Osr1 acts downstream of and interacts synergistically with Six2 to maintain nephron progenitor cells during kidney organogenesis. *Development* 2014; 141: 1442–1452. [PubMed: 24598167]
20. Huang L, Mokkupati S, Hu Q, et al. Nephron Progenitor But Not Stromal Progenitor Cells Give Rise to Wilms Tumors in Mouse Models with beta-Catenin Activation or Wt1 Ablation and Igf2 Upregulation. *Neoplasia* 2016; 18: 71–81. [PubMed: 26936393]
21. Combes AN, Lefevre JG, Wilson S, et al. Cap mesenchyme cell swarming during kidney development is influenced by attraction, repulsion, and adhesion to the ureteric tip. *Developmental biology* 2016; 418: 297–306. [PubMed: 27346698]
22. Combes AN, Short KM, Lefevre J, et al. An integrated pipeline for the multidimensional analysis of branching morphogenesis. *Nature protocols* 2014; 9: 2859–2879. [PubMed: 25411953]
23. Boyle S, Shioda T, Perantoni AO, et al. Cited1 and Cited2 are differentially expressed in the developing kidney but are not required for nephrogenesis. *Developmental dynamics : an official publication of the American Association of Anatomists* 2007; 236: 2321–2330. [PubMed: 17615577]
24. Brunskill EW, Potter SS. RNA-Seq defines novel genes, RNA processing patterns and enhancer maps for the early stages of nephrogenesis: Hox supergenes. *Developmental biology* 2012; 368: 4–17. [PubMed: 22664176]
25. Karner CM, Das A, Ma Z, et al. Canonical Wnt9b signaling balances progenitor cell expansion and differentiation during kidney development. *Development* 2011; 138: 1247–1257. [PubMed: 21350016]
26. Motamedi FJ, Badro DA, Clarkson M, et al. WT1 controls antagonistic FGF and BMP-pSMAD pathways in early renal progenitors. *Nature communications* 2014; 5: 4444.
27. Rumballe BA, Georgas KM, Combes AN, et al. Nephron formation adopts a novel spatial topology at cessation of nephrogenesis. *Developmental biology* 2011; 360: 110–122 [PubMed: 21963425]
28. Chen J, Bardes EE, Aronow BJ, et al. ToppGene Suite for gene list enrichment analysis and candidate gene prioritization. *Nucleic acids research* 2009; 37: W305–311. [PubMed: 19465376]
29. Relaix F, Demignon J, Laclef C, et al. Six homeoproteins directly activate Myod expression in the gene regulatory networks that control early myogenesis. *PLoS genetics* 2013; 9: e1003425. [PubMed: 23637613]
30. MacArthur DG, Seto JT, Raftery JM, et al. Loss of ACTN3 gene function alters mouse muscle metabolism and shows evidence of positive selection in humans. *Nature genetics* 2007; 39: 1261–1265. [PubMed: 17828264]
31. Wu D, Smyth GK. Camera: a competitive gene set test accounting for inter-gene correlation. *Nucleic acids research* 2012; 40: e133. [PubMed: 22638577]

32. Xu J, Wong EY, Cheng C, et al. Eya1 interacts with Six2 and Myc to regulate expansion of the nephron progenitor pool during nephrogenesis. *Developmental cell* 2014; 31: 434–447. [PubMed: 25458011]
33. Claveria C, Giovinazzo G, Sierra R, et al. Myc-driven endogenous cell competition in the early mammalian embryo. *Nature* 2013; 500: 39–44. [PubMed: 23842495]
34. Moreno E, Basler K. dMyc transforms cells into super-competitors. *Cell* 2004; 117: 117–129. [PubMed: 15066287]
35. Birket MJ, Ribeiro MC, Verkerk AO, et al. Expansion and patterning of cardiovascular progenitors derived from human pluripotent stem cells. *Nature biotechnology* 2015; 33: 970–979.
36. Couillard M, Trudel M. C-myc as a modulator of renal stem/progenitor cell population. *Developmental dynamics : an official publication of the American Association of Anatomists* 2009; 238: 405–414. [PubMed: 19161241]
37. Mukasa A, Wykosky J, Ligon KL, et al. Mutant EGFR is required for maintenance of glioma growth in vivo, and its ablation leads to escape from receptor dependence. *Proceedings of the National Academy of Sciences of the United States of America* 2010; 107: 2616–2621. [PubMed: 20133782]
38. Piascik MT, Perez DM. Alpha1-adrenergic receptors: new insights and directions. *The Journal of pharmacology and experimental therapeutics* 2001; 298: 403–410. [PubMed: 11454900]
39. Weber S, Taylor JC, Winyard P, et al. SIX2 and BMP4 mutations associate with anomalous kidney development. *Journal of the American Society of Nephrology : JASN* 2008; 19: 891–903. [PubMed: 18305125]
40. Faguer S, Chassaing N, Bandin F, et al. Should SIX2 be routinely tested in patients with isolated congenital abnormalities of kidneys and/or urinary tract (CAKUT)? *European journal of medical genetics* 2012; 55: 688–689. [PubMed: 22809486]
41. Hwang DY, Dworschak GC, Kohl S, et al. Mutations in 12 known dominant disease-causing genes clarify many congenital anomalies of the kidney and urinary tract. *Kidney international* 2014; 85: 1429–1433. [PubMed: 24429398]
42. Huh SH, Jones J, Warchol ME, et al. Differentiation of the lateral compartment of the cochlea requires a temporally restricted FGF20 signal. *PLoS biology* 2012; 10: e1001231. [PubMed: 22235191]
43. Cullen-McEwen LA, Armitage JA, Nyengaard JR, et al. A design-based method for estimating glomerular number in the developing kidney. *American journal of physiology Renal physiology* 2011; 300: F1448–1453. [PubMed: 21411478]
44. Dobin A, Davis CA, Schlesinger F, et al. STAR: ultrafast universal RNA-seq aligner. *Bioinformatics* 2013; 29: 15–21. [PubMed: 23104886]
45. Liao Y, Smyth GK, Shi W. featureCounts: an efficient general purpose program for assigning sequence reads to genomic features. *Bioinformatics* 2014; 30: 923–930. [PubMed: 24227677]
46. Robinson MD, Oshlack A. A scaling normalization method for differential expression analysis of RNA-seq data. *Genome biology* 2010; 11: R25. [PubMed: 20196867]
47. Ritchie ME, Phipson B, Wu D, et al. limma powers differential expression analyses for RNA-sequencing and microarray studies. *Nucleic acids research* 2015; 43: e47. [PubMed: 25605792]
48. Smyth GK, Michaud J, Scott HS. Use of within-array replicate spots for assessing differential expression in microarray experiments. *Bioinformatics* 2005; 21: 2067–2075. [PubMed: 15657102]

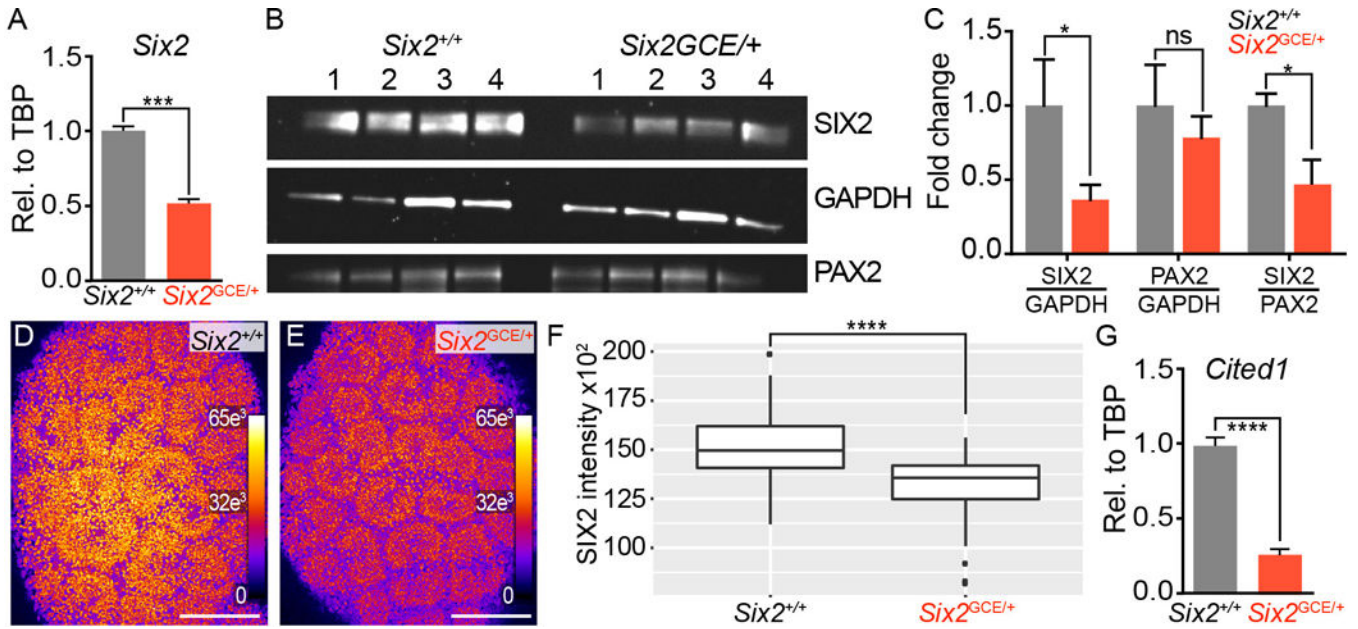


Figure 1). Validation of haploinsufficiency and compromised progenitor state

A) *Six2* mRNA is reduced by 50% in *Six2*^{GCE/+} compared to *Six2*^{+/+} at 15.5 dpc. Data is the average of three biological replicates from each genotype, $p=0.0003$. mRNA levels expressed relative to *Six2*^{+/+}. **B)** Western blot bands for SIX2, GAPDH, and PAX2 at 15.5 dpc with four biological replicates per genotype. See Supplementary Figure 1 for full gels. **C)** Densitometry analysis showing reduced SIX2 relative to GAPDH ($p=0.014$), no change in PAX2 relative to GAPDH ($p=0.256$), reduced SIX2 relative to PAX2 ($p=0.049$). Data represents the average of 4 biological replicates. **D&E)** Pseudocoloured map of SIX2 intensity in representative *Six2*^{+/+} and *Six2*^{GCE/+} samples imaged and displayed on the same settings. Colour scale indicates fluorescence intensity units. Scale bar 100 μ m. **F)** Box and whisker plot of mean SIX2 intensity per cap cluster for *Six2*^{+/+} ($n=104$) vs *Six2*^{GCE/+} ($n=55$), two sample t-test with welch's correction $p=6.4e-10$. **G)** *Cited1* mRNA levels are dramatically reduced in the *Six2*^{GCE/+} compared to *Six2*^{+/+} ($p=0.00005$). Error bars on all graphs represent SEM, p values from two-tailed t-tests with Welch's correction.

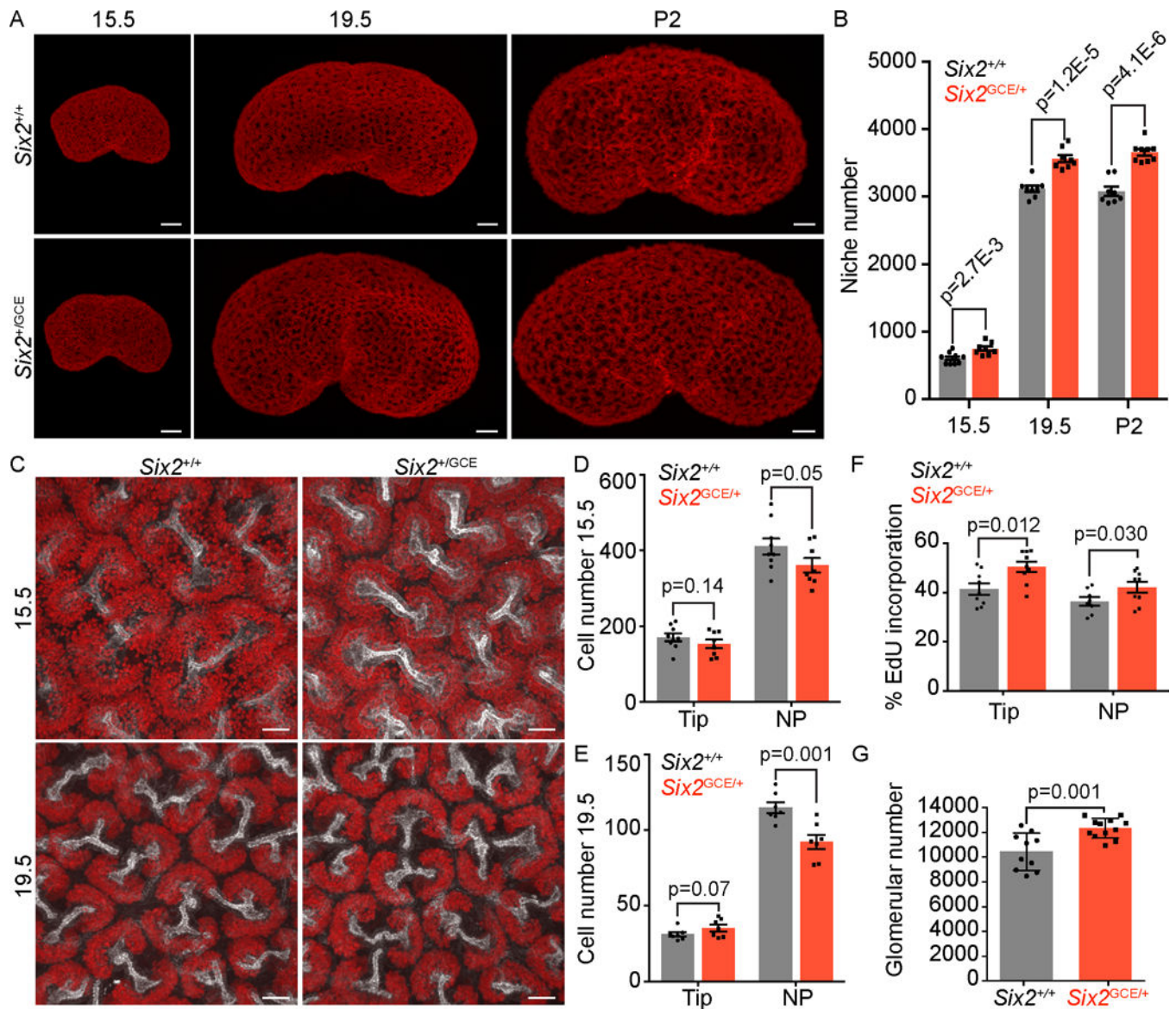


Figure 2). Increased branching, tip proliferation, and nephron endowment in *Six2*^{GCE/+}.

A) Whole organ OPT of SIX2-antibody stained *Six2*^{+/+} and *Six2*^{GCE/+} kidneys at 15.5 dpc, 19.5 dpc, and P2. Scale 300 μ m for all. Exposures were optimised for each sample hence signal intensity should not be compared between images. **B)** Niche counts from OPT data for 15.5 dpc (n = 9 *Six2*^{+/+}, 8 *Six2*^{GCE/+}), 19.5 dpc (n = 8 *Six2*^{+/+}, 8 *Six2*^{GCE/+}), and P2 (n = 8 *Six2*^{+/+}, 9 *Six2*^{GCE/+}). **C)** Max. intensity projection confocal data from 15.5 dpc and 19.5 dpc *Six2*^{+/+} and *Six2*^{GCE/+} kidneys stained with SIX2 (red) and CYTOK (white). Scale bars 30 μ m. Exposures were optimised for each sample hence signal intensity should not be compared between images. **D)** Tip and cap cell number at 15.5 dpc. Each data point represents average cell number per niche in an individual sample; Sample numbers = 9 *Six2*^{+/+}, 8 *Six2*^{GCE/+}. **E)** Tip and cap cell number at 19.5 dpc. Points as per D, n= 9 *Six2*^{+/+}, 8 *Six2*^{GCE/+}. **F)** % EdU incorporation for tip and cap cell populations at 13.5 dpc, 30 minutes after exposure to EdU. Each data point represents % incorporation per sample, data

derives from three replicate experiments; n = 8 *Six2*^{+/+}, 9 *Six2*^{GCE/+}. **G**) Comparison of estimated glomerular number between P21 (adult) *Six2*^{+/+} and *Six2*^{GCE/+} by stereology; n= 10 *Six2*^{+/+}, 12 *Six2*^{GCE/+}. Error bars in all graphs represent SEM, p values determined by 1-tailed t-test with Welch's correction.

Author Manuscript

Author Manuscript

Author Manuscript

Author Manuscript

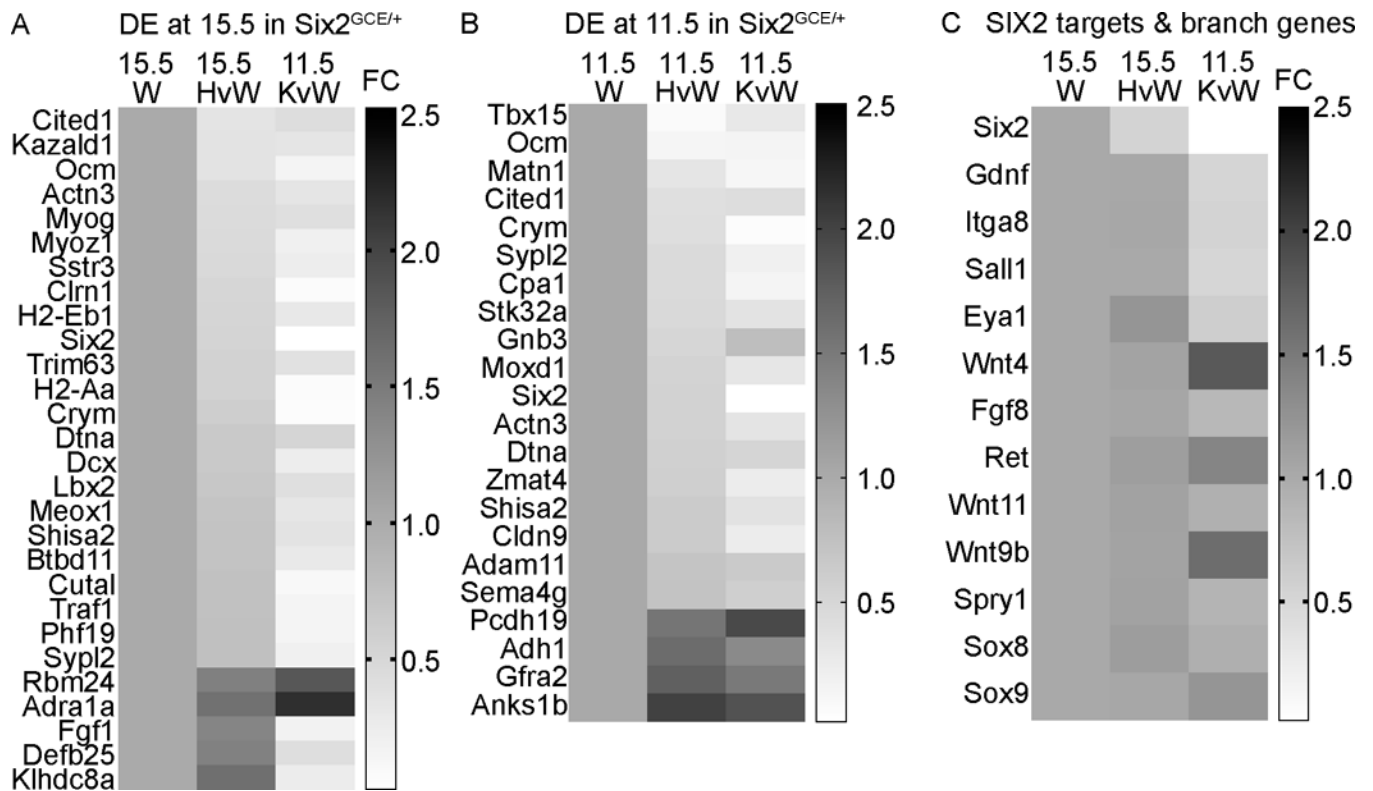


Figure 3). Gene expression changes in the *Six2*^{GCE/+} kidney.

A) Genes differentially expressed (DE) at -0.4 or 0.4 LogFC of *Six2*^{+/+} values at 15.5dpc in *Six2*^{GCE/+} and -1 or 1 LogFC of wildtype in 11.5 dpc *Six2*^{GCE/GCE}; adjusted $p < 0.05$ for all. Key indicates fold change in expression compared to wildtype for all panels. For all panels, W= wildtype/*Six2*^{+/+}; H= heterozygous/*Six2*^{GCE/+}; K= knockout/*Six2*^{GCE/GCE}. **B)** Genes expressed at -0.4 or 0.4 LogFC of wildtype values at 11.5dpc in *Six2*^{GCE/+} and -1 or 1 LogFC of wildtype in *Six2*^{GCE/GCE} adjusted $p < 0.05$. **C)** Examples of gene expression for some established SIX2 targets and branching genes in *Six2*^{GCE/+} and *Six2*^{GCE/GCE}; Aside from *Six2*, none of these changes were statistically significant in the *Six2*^{GCE/+}.

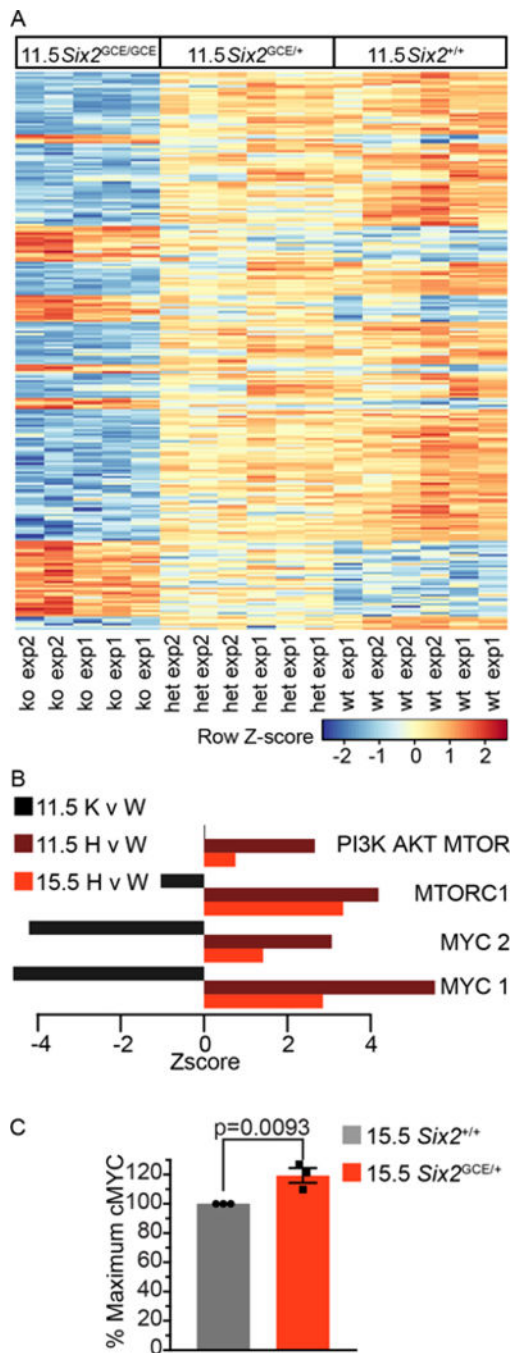


Figure 4). Analysis of transcriptional changes

A) Unsupervised clustering of the top 250 differentially expressed genes between 11.5 dpc *Six2*^{GCE/GCE} and *Six2*^{+/+}. Each row represents a gene, each column an independent sample. Colour indicates normalised expression (Z-score) blue is low, red high. **B)** Gene set testing reveals an upregulation of pathways associated with growth (MYC targets V1 and V2), progenitor maintenance (mTOR, mTORC1 signalling), and differentiation (PI3K signalling) in *Six2*^{GCE/+}. The pathways associated with MYC and mTORC1 are downregulated in

Six2^{GCE/GCE}. **D**) MYC protein levels are significantly increased in the *Six2*^{GCE/+}. Points represent average values from three independent litters. Unpaired t test.

Author Manuscript

Author Manuscript

Author Manuscript

Author Manuscript

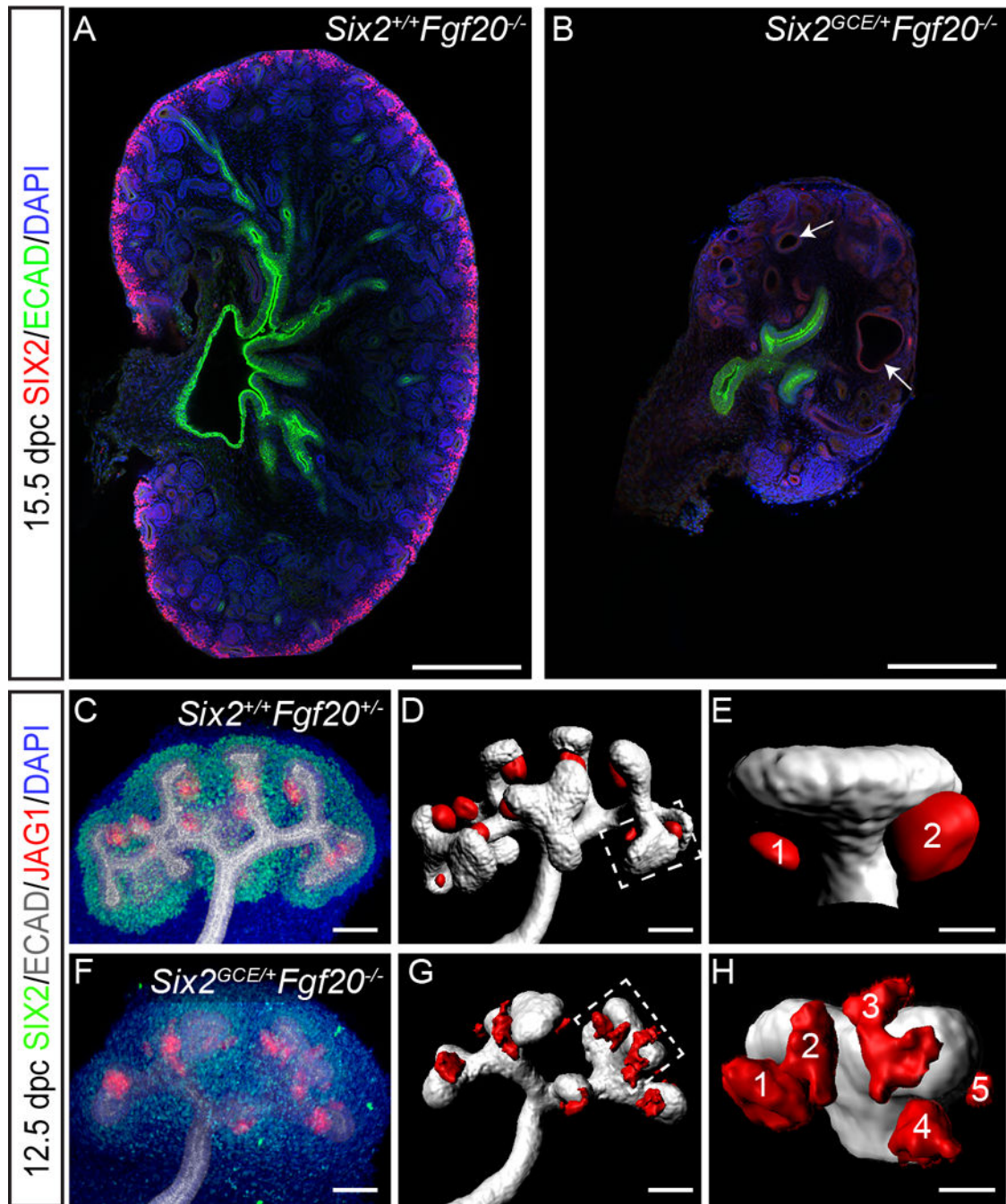


Figure 5). Cap mesenchyme lacking one copy of *Six2* undergoes premature differentiation in the absence of *Fgf20*.

A) Staining of the CM (SIX2, red), ureteric tree (ECAD, green), and nuclei (DAPI, blue) in a 15.5 dpc *Six2*^{+/+}*Fgf20*^{-/-} kidney. Scale 200µm. **B)** Nephron progenitors exhaust before 15.5 dpc in *Six2*^{GCE/+}*Fgf20*^{-/-} kidneys. Dilated nephrons are observed (arrows) and the ureteric tree is underdeveloped. Staining and scale as per A. **C)** Maximum intensity projection of the CM (SIX2, green), tree (ECAD, grey), renal vesicles (JAG1, red), and nuclei (DAPI, blue) in a 12.5 dpc *Six2*^{+/+}*Fgf20*^{-/-} kidney, scale 50µm. **D)** Rendering of the

tree (grey) and renal vesicles (red) from C, scale 50 μ m. **E)** Zoom of boxed region in E shows t-stage tip with two renal vesicles attached on medullary side, scale 20 μ m. **F)** 12.5 dpc *Six2*^{GCE/+}*Fgf20*^{-/-} kidney as per C, scale 50 μ m. **G)** Rendering from F, scale 50 μ m. **H)** Zoom of region in G showing t-stage tip with 5 renal vesicles, 2 in ectopic positions, scale 20 μ m.

Author Manuscript

Author Manuscript

Author Manuscript

Author Manuscript